

First-Order Contaminant Removal in the Hyporheic Zone of Streams: Physical Insights from a Simple Analytical Model

Stanley B. Grant,^{*,†,‡,||} Keith Stolzenbach,[§] Morvarid Azizian,[‡] Michael J. Stewardson,^{||} Fulvio Boano,[⊥] and Laura Bardini[⊥]

[†]Department of Civil and Environmental Engineering, Henry Samueli School of Engineering, University of California, Irvine, California 92697, United States

[‡]Department of Chemical Engineering and Materials Science, Henry Samueli School of Engineering, University of California, Irvine, California 92697, United States

[§]Department of Civil and Environmental Engineering, Henry Samueli School of Engineering and Applied Science, University of California, Los Angeles, California 90095, United States

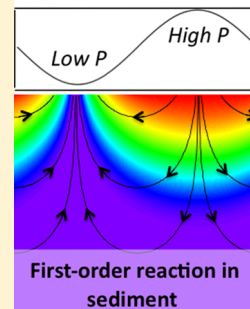
^{||}Department of Infrastructure Engineering, Melbourne School of Engineering, The University of Melbourne, Victoria 3010, Australia

[⊥]Department of Environment, Land and Infrastructure Engineering, Politecnico di Torino, Corso Duca degli Abruzzi 24, Turin, Italy

S Supporting Information

ABSTRACT: A simple analytical model is presented for the removal of stream-borne contaminants by hyporheic exchange across duned or rippled streambeds. The model assumes a steady-state balance between contaminant supply from the stream and first-order reaction in the sediment. Hyporheic exchange occurs by bed form pumping, in which water and contaminants flow into bed forms in high-pressure regions (downwelling zones) and out of bed forms in low-pressure regions (upwelling zones). Model-predicted contaminant concentrations are higher in downwelling zones than upwelling zones, reflecting the strong coupling that exists between transport and reaction in these systems. When flow-averaged, the concentration difference across upwelling and downwelling zones drives a net contaminant flux into the sediment bed proportional to the average downwelling velocity. The downwelling velocity is functionally equivalent to a mass transfer coefficient, and can be estimated from stream state variables including stream velocity, bed form geometry, and the hydraulic conductivity and porosity of the sediment. Increasing the mass transfer coefficient increases the fraction of streamwater cycling through the hyporheic zone (per unit length of stream) but also decreases the time contaminants undergo first-order reaction in the sediment. As a consequence, small changes in stream state variables can significantly alter the performance of hyporheic zone treatment systems.

Dynamic pressure at the sediment-water interface



can significantly alter the

INTRODUCTION

The hyporheic zone is the region beneath and adjacent to a stream where surface water and groundwater mix. Its physical and chemical environment supports a community of organisms that collectively remove contaminants and cycle carbon, energy, and nutrients.^{1,2} The hyporheic zone also regulates stream temperature and sediment budgets, serves as a spawning ground/refuge for fish species, and provides a rooting zone for aquatic plants. These ecosystem services require vigorous exchange of water, nutrients and energy across the sediment–water interface, a process referred to as hyporheic exchange. Stream restoration can include features—such as pools, riffles, steps, debris dams, bars, meander bends, and side channels—that enhance hyporheic exchange.³ Hyporheic exchange can also be incorporated into the design of engineered streams to facilitate the removal of carbon, phosphorus, nitrogen, and other contaminants from polluted waters. In arid urban settings, for example, dry streambeds can be converted to hyporheic zone treatment systems for polishing effluent from wastewater treatment plants.⁴ Potential benefits include improved receiving water quality, groundwater protection, new stream habitat, low

energy consumption, and a small carbon footprint. On the other hand, a poorly managed hyporheic zone can degrade surface water quality, for example by polluting the overlying water column with fecal bacteria growing in the sediment bed⁵ or releasing heavy metals and nutrients.⁶ Whether the goal is restoring natural streams, engineering low-energy treatment systems, or managing existing water quality impairments, quantitative tools are needed to predict the effects of hyporheic exchange on the transport and transformation of contaminants in streams.

Here we focus on a particular type of hyporheic exchange that occurs when a turbulent stream flows over bed forms (such as ripples and dunes) on a permeable sediment bed. The central role of turbulence in this problem poses special (multiphysics) challenges that set it apart from other low-energy treatment systems where the bulk flow is often laminar or transitionally turbulent, such as surface⁷ and subsurface⁸ wetlands. The present

Received: April 5, 2014

Revised: July 14, 2014

Accepted: September 2, 2014

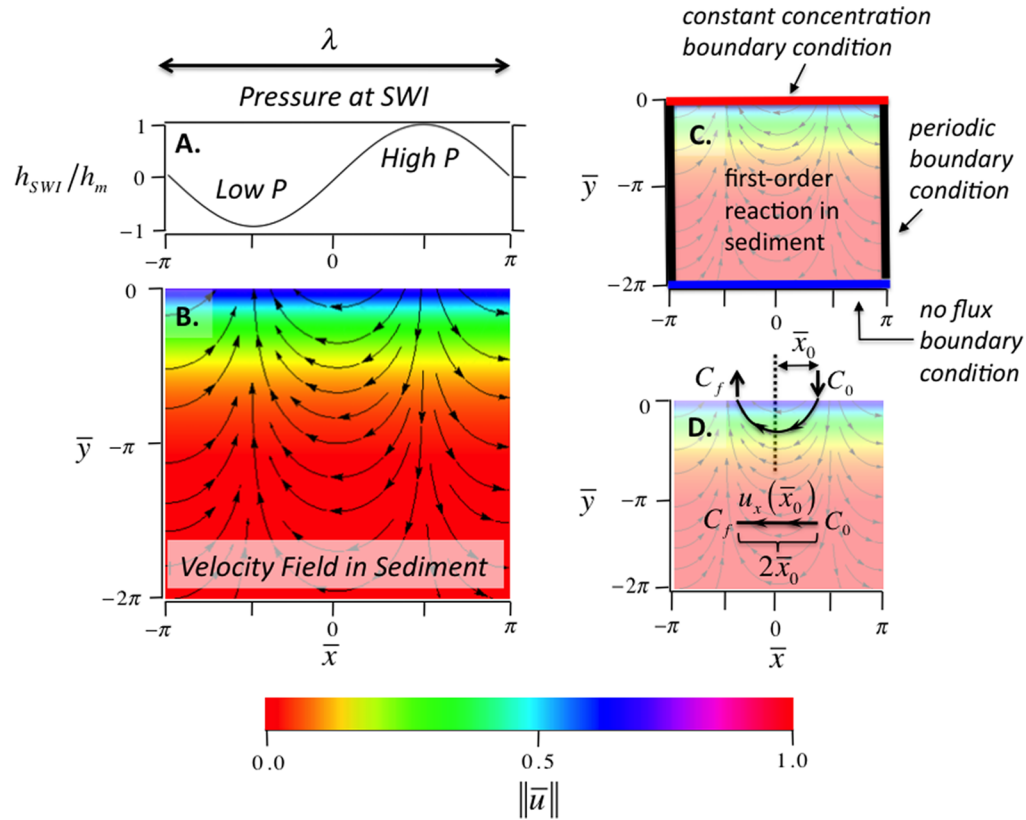


Figure 1. Elliott and Brooks (EB) model for flow through the hyporheic zone of a stream with bed forms, including the assumed pressure head distribution at the sediment–water interface (SWI, panel A) and the derived velocity field in the hyporheic zone (panel B). Flow from the stream into the sediment (downwelling) occurs in high-pressure regions; flow from the stream into the sediment (upwelling) occurs in low-pressure regions. The color denotes the modulus of the Darcy flux vector (see eq (2d)). Horizontal and vertical distances are reduced by the wavelength λ of a bed form: $\bar{x} = 2\pi x/\lambda$ and $\bar{y} = 2\pi y/\lambda$. Contaminant transport and first-order reaction in the hyporheic zone can be modeled numerically (assuming that mass transfer in the sediment occurs by advection, mechanical dispersion, and molecular diffusion) (panel C) or with an analytical solution (assuming that mass transfer in the sediment occurs only by advection) (panel D).

state-of-the-art involves three steps (e.g., refs 9–11): (1) calculating the pressure distribution at the sediment–water interface by numerically solving the Navier–Stokes equations for turbulent streamflow over the bed forms of interest; (2) calculating water flow through the hyporheic zone from Darcy’s Law and the continuity equation using pressure distributions along the sediment–water interface (from step (1)) and stream-aquifer boundary together with an assumed sediment permeability field; and (3) calculating solute concentrations in the interstitial fluids of the sediment from a mass conservation equation that accounts for physical transport processes (advection, mechanical dispersion, molecular diffusion) and the chemical and biogeochemical transformations of interest. To complement this relatively computationally- and data-intensive numerical approach, in this paper we derive and solve a simple analytical model of hyporheic exchange and in-sediment reaction. Our simple model builds on an idealized flow field for hyporheic exchange first proposed by Elliott and Brooks (hereafter referred to as EB)^{12,13} and generalizes a solution for hyporheic exchange and reaction presented by Rutherford et al. that focused on benthic oxygen uptake of sediments in a polluted stream.¹⁴

The Elliott and Brooks Model for Pumping Across Bed forms. The EB flow model is premised on the idea that turbulent flow over periodic bed forms causes the dynamic pressure at the sediment–water interface to oscillate with distance downstream. Pressure variation is caused by acceleration of flow and detachment of the velocity boundary layer over the crest of the bed

form.^{15,16} The resulting stream-parallel pressure oscillation drives flow across the sediment–water interface, into the sediment in high-pressure regions (downwelling) and out of the sediment in low-pressure regions (upwelling). In the EB flow model, this periodic pressure variation at the sediment–water interface is idealized as a sinusoidal function, where the variable h_{SWI} (units of length, L) refers to pressure head (i.e., pressure normalized by the specific weight of water) (Figure 1A):

$$h_{SWI} = h_m \sin(\bar{x}) \tag{1}$$

Variables in eq 1 include the reduced horizontal coordinate $\bar{x} = 2\pi x/\lambda$ [–], the horizontal coordinate parallel to the sediment–water interface x [L], and the wavelength λ [L] and amplitude h_m [L] of the pressure head variation. The wavelength λ of the pressure wave corresponds to the wavelength of the bed form, and the trough and peak of the pressure wave correspond to where the velocity boundary layer detaches (at the bed form crest) and reattaches (on the lee side of the bed form), respectively.

Assuming a sinusoidal pressure distribution h_{SWI} at the sediment–water interface and constant hydraulic conductivity K_h (units of length per time, $L T^{-1}$) throughout the sediment bed, application of Darcy’s Law and the continuity equation yields the following solution for the pressure head and velocity field in the interstitial pores of the hyporheic zone:¹²

$$\bar{h}(\bar{x}, \bar{y}) = h/h_m = \sin \bar{x} e^{\bar{y}} \tag{2a}$$

$$\bar{u}_x = u_x/u_m = -\cos \bar{x}e^{\bar{y}} \quad (2b)$$

$$\bar{u}_y = u_y/u_m = -\sin \bar{x}e^{\bar{y}} \quad (2c)$$

$$\|\bar{u}\| = \sqrt{\bar{u}_x^2 + \bar{u}_y^2} = e^{\bar{y}} \quad (2d)$$

$$\bar{x} = 2\pi x/\lambda \quad (2e)$$

$$\bar{y} = 2\pi y/\lambda \quad (2f)$$

$$u_m = 2\pi K_h h_m/\lambda \quad (2g)$$

The vertical distance above the sediment–water interface is denoted by the coordinate y [L]. The variables u_x [L T⁻¹], u_y [L T⁻¹], and $\|\bar{u}\|$ [-] represent, respectively, the x -component, y -component, and a reduced form of the modulus of the Darcy flux (flow volume per unit area) through the sediment. Application of the EB flow model requires an estimate for either the maximum Darcy velocity u_m [L T⁻¹] or pressure head amplitude h_m . These parameters can be estimated from stream state variables using one of several empirical relationships, detailed later.

There are two striking features of the velocity field predicted by the EB flow model (Figure 1B). First, circulation of water across the sediment–water interface occurs in a series of identical (or mirror-image) unit cells; a single unit cell extends from $\bar{x} = -\pi/2$ to $\bar{x} = \pi/2$ in Figure 1B. Second, the modulus of the Darcy velocity vector decays exponentially with depth (eq 2d, see color in Figure 1B; note that the vertical coordinate y is oriented upwards, and therefore y is negative into the streambed). These two features of the EB flow field—its unit cell structure and exponential decline with depth—are qualitatively similar to numerical predictions of in-sediment circulation patterns generated by turbulent flow over asymmetrical dunes (e.g., see Figure 1 in ref 15) and experimental observations of streaklines through sediment during hyporheic exchange.^{13,16} The depth to which the velocity field extends into the sediment bed (1/e-folding depth approximately equal to λ) also agrees well with experimental measurements and numerical simulations of hyporheic exchange under dunes, $d_{\text{HZ}} \approx a\lambda$, where d_{HZ} [L] is the depth of the hyporheic zone and the constant a varies between 0.4 and 0.7 depending on dune geometry.^{11,15}

A potential limitation of the EB model is its assumption that the sediment–water interface is flat. To explore this potential limitation, we compared the modulus of the Darcy flux predicted by the EB model (eq 2d) with the Darcy flux simulated using the approach outlined earlier; namely, solving

$$\mathbf{D} = \begin{bmatrix} \frac{u_m e^{\bar{y}}}{\theta} (\alpha_L \cos^2 \bar{x} + \alpha_T \sin^2 \bar{x}) + D'_m & \frac{u_m e^{\bar{y}}}{\theta} (\alpha_L - \alpha_T) \frac{\sin 2\bar{x}}{2} \\ \frac{u_m e^{\bar{y}}}{\theta} (\alpha_L - \alpha_T) \frac{\sin 2\bar{x}}{2} & \frac{u_m e^{\bar{y}}}{\theta} (\alpha_L \sin^2 \bar{x} + \alpha_T \cos^2 \bar{x}) + D'_m \end{bmatrix} \quad (4b)$$

Variables appearing here include the dispersivities parallel α_L [L] and transverse α_T [L] to the streamlines, and the molecular diffusion coefficient of solute in water D_m [L² T⁻¹] modified by a tortuosity parameter β [-] that takes into account the twists and turns associated with diffusion through connected pore spaces in the sediment: $D'_m = \beta D_m$ where $\beta = (1 + 3(1 + \theta))^{-1}$.¹⁷ As is common for these types of analyses (e.g., refs 9 and 11), our model does not consider variations in the permeability field, and exchange between so-called mobile and immobile zones in

the Navier–Stokes equation for turbulent flow over a bed form, and then solving flow through the hyporheic zone by application of Darcy’s equation and the continuity equation (see Supporting Information (SI)). Below the base of the bed form the modulus of the Darcy flux predicted by the numerical solution exhibits the same functional behavior as EB’s flat-bed solution (i.e., both solutions decay exponentially with depth). As might be expected, the functional form of the two solutions differs for elevations between the base and crest of the bed form (SI Figure S2). The surface-averaged Darcy flux across the sediment–water interface is also similar (within about 11%, see SI). In summary, given its simplicity and relative consistency with both experimental observations and numerical simulations, the EB velocity field is an excellent starting point for the modeling described next.

Numerical Simulation of Contaminant Removal in the Hyporheic Zone. To illustrate how the EB velocity field affects mass transport and reaction in the hyporheic zone, we carried out a series of numerical simulations. For these simulations the following boundary conditions were adopted:⁹ (1) constant concentration at the top boundary ($C = C_0$ at $\bar{y} = 0$, red line in Figure 1C), (2) a no-flux condition at the bottom boundary ($\partial C/\partial \bar{y} = 0$ at $\bar{y} = -2\pi$, blue line in Figure 1C); and (3) periodic boundaries at the edges (matching concentrations and fluxes at $\bar{x} = \pm \pi$, black lines in Figure 1C). At every point in the numerical domain we assumed a steady-state balance between first-order reaction in the sediment and contaminant supply from the stream:⁹

$$\nabla \cdot \left(\frac{\mathbf{u}}{\theta} C - \mathbf{D} \cdot \nabla C \right) = -k_r C \quad (3)$$

Equation 3 accounts for transport and mixing through the hyporheic zone by advection, mechanical dispersion, and molecular diffusion (two terms on left-hand side) and removal within the sediment by first-order reaction (term on right-hand side). The variables C (mass per volume [M L⁻³]), θ [-], \mathbf{u} [L T⁻¹], \mathbf{D} [L² T⁻¹], and k_r [T⁻¹] represent contaminant concentration in the sediment’s interstitial pores, sediment porosity, Darcy flux vector, dispersion/diffusion tensor, and first-order rate constant for contaminant removal, respectively. According to the EB velocity field (eqs 2b and 2c) the Darcy velocity vector and the dispersion/diffusion tensor (see⁹) can be written as follows:

$$\mathbf{u} = -u_m \cos \bar{x} e^{\bar{y}} \hat{i} - u_m \sin \bar{x} e^{\bar{y}} \hat{j} \quad (4a)$$

the sediment. However, a recent numerical study found that, under the steady-state conditions employed here, small-scale heterogeneities in the permeability field have relatively little effect on the overall reaction rates observed within the streambed.¹⁸

Equations 4a and 4b were substituted into eq 3 and the resulting partial differential equation was solved using a generic multiphysics finite element solver with adaptive meshing and error control (COMSOL, version 4.4). The parameter values

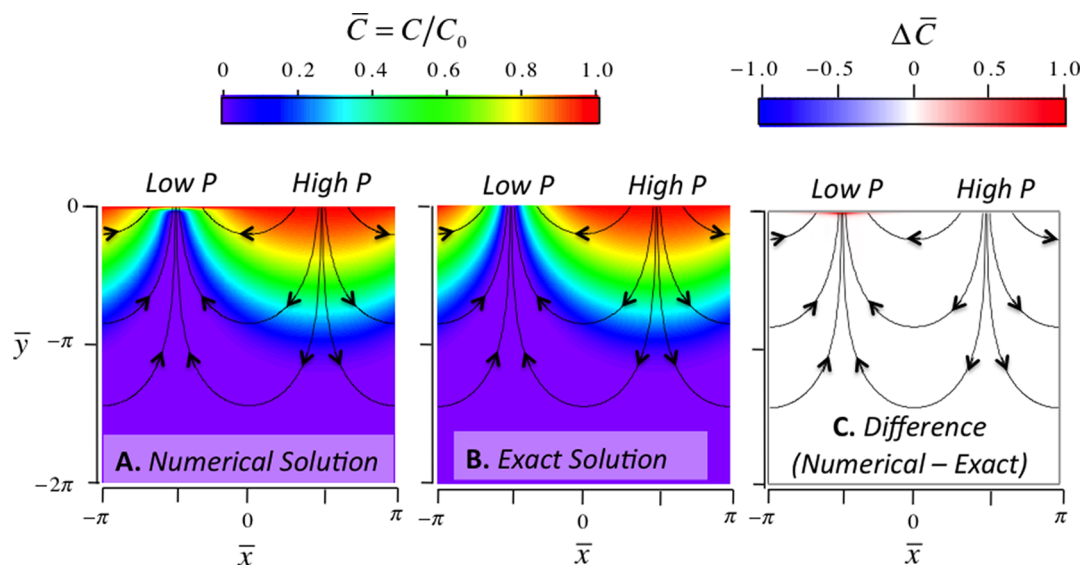


Figure 2. Concentration fields predicted by the numerical (panel A) and analytical (panel B) solutions of hyporheic exchange and first-order reaction, assuming flow through the hyporheic zone follows the EB velocity model (see Figure 1). The colors in panel A and B denote the concentration of contaminant in the pore fluid C normalized by the concentration of contaminant in the stream (C_0): $\bar{C} = C/C_0$. The difference between numerical and exact solutions ($\Delta\bar{C} = \bar{C}_{\text{numerical}} - \bar{C}_{\text{exact}}$) is shown in Panel C.

utilized for this numerical simulation (SI Table 1) were taken from a previously published modeling study of hyporheic exchange;⁹ they are representative of a medium-sized stream flowing over periodic dunes on a permeable bed of well-sorted sand. The first-order rate constant corresponds to a contaminant half-life of 1.6 days, which is typical for the respiration of dissolved organic carbon in a stream⁹ or the mineralization of a low persistence anthropogenic contaminant, such as the pharmaceutical compound paracetamol, in a sediment/water matrix under environmentally relevant conditions.¹⁹

Contaminant concentrations predicted by the numerical simulation vary dramatically across the upwelling and downwelling zones of the bed form (Figure 2A). In the downwelling (high pressure) zone, contaminant-rich water penetrates approximately half a dune wavelength into the sediment ($\bar{y} \approx -\pi$). In the upwelling (low pressure) zone contaminant-depleted waters extend nearly all the way to the surface ($\bar{y} \approx 0$). For the steady-state form of the mass balance equation adopted here (eq 3), the mass of contaminant crossing the sediment–water interface exactly balances the mass removed in the hyporheic zone by first-order reaction. Under such conditions, the average flux across the sediment–water interface can be calculated as follows: $J = \theta C_{\text{ave}} k_r d_{\text{CD}}$ [$\text{M L}^{-2} \text{T}^{-1}$] where C_{ave} is the average contaminant concentration in the computational domain, k_r is the first-order reaction rate, θ is streambed porosity, and d_{CD} is the depth of the computational domain. Here and throughout the remainder of the paper, J is defined as the mass transported per unit streambed area (including both sediment matrix and pore spaces) per time; the negative sign denotes mass transport into the sediment bed (i.e., in the direction opposite of the y -axis which is oriented upwards, see Figure 1B). In our numerical simulation the first-order reaction rate is $k_r = 5 \times 10^{-6} \text{ s}^{-1}$, the depth of the computational domain is $d_{\text{CD}} = \lambda = 1 \text{ m}$, $\theta = 0.4$, and $C_{\text{ave}} = 0.206C_0$ where C_0 is the fixed concentration of contaminant in the stream. Therefore, the flux of contaminant across the sediment–water interface for this particular numerical simulation is $J = -(4 \times 10^{-7} \text{ ms}^{-1})C_0$.

Relative Importance of Advection, Mechanical Dispersion, And Molecular Diffusion.

The numerical simulation used to generate Figure 2A includes all three transport mechanisms potentially operative in the hyporheic zone; namely, advection, mechanical dispersion, and molecular diffusion. An order-of-magnitude analysis suggests that, for the set of parameters listed in SI Table 1, mass transport in the hyporheic zone is dominated by advection (see SI). To test this idea, we carried out a series of numerical simulations in which different combinations of transport mechanisms were turned on or off. Three scenarios were tested: (1) all three transport mechanisms turned-on (i.e., the simulation used to generate Figure 2A); (2) advection and mechanical dispersion turned-on and molecular diffusion turned-off; and (3) advection and molecular diffusion turned-on and mechanical dispersion turned-off. The obvious fourth scenario (both mechanical dispersion and molecular diffusion turned-off) could not be run because of an artifact associated with the surface boundary condition; this artifact will be discussed in the next section. For the three scenarios, the concentration fields are indistinguishable (Figure S3 in SI) and the flux (J) across the sediment–water interface is the same to within three significant digits. Because the concentration field is unchanged when mechanical dispersion is substituted for molecular diffusion (and vice versa), we conclude that the order-of-magnitude analysis is correct: mass transport within the hyporheic zone is dominated by advection in this case. More generally, when a contaminant is removed by first-order reaction in the sediment bed, advection will dominate over mechanical dispersion when $\alpha_L k_r \theta / u_m \ll 1$; advection will dominate over molecular diffusion when $\theta \beta D_m k_r / u_m^2 \ll 1$ (see SI for derivations).

Artifacts Associated with the Surface Boundary Condition.

In numerical simulations of hyporheic exchange and reaction it is common to apply a constant concentration (i.e., a Dirichlet or first-type) boundary condition $C = C_0$ at the sediment–water interface (e.g., refs 9, 18, 20), as was the case for the numerical simulation described in the last section. As is evident from Figure 1B, flow fields in the downwelling and

upwelling zones are symmetrical. For a constant concentration boundary condition at the surface, the advective mass flow into the sediment must equal the advective mass flow out of the sediment. If advection dominates over dispersion and diffusion, then mass loss by reaction will cause concentration to decrease along a streamline, from the initial value of C_0 in the downwelling zone to the upwelling zone where the concentration rapidly rebounds to C_0 at the sediment-water interface. Total mass conservation is achieved by dispersive and/or diffusive mass transport into the sediment due to the steep concentration gradient at the sediment-water interface (see SI). This explains why the fourth scenario described in the last section (both mechanical dispersion and molecular diffusion turned-off) could not be simulated—in numerical simulations of hyporheic exchange in which a constant concentration boundary condition is applied at the sediment–water interface, overall mass balance cannot be satisfied without including some form of Fickian diffusion/dispersion.

Analytical Model of Hyporheic Exchange: Mass-Transfer-Limit Solution. In this section we derive an exact solution for mass flux across the sediment-water interface under mass-transfer limited conditions. We focus on a single streamline; namely, the one that intersects the sediment-water interface at $x = x_0$ (top highlighted streamline, Figure 1D). Along this particular streamline and assuming mass transport occurs by advection alone (i.e., mechanical dispersion and molecular diffusion are neglected, see last section), mass flows into the hyporheic zone at a rate of $dm_{in}(x_0) = |C_0 W u_y(x = x_0, y = 0) dx_0|$ and out of the hyporheic zone at a rate of $dm_{out}(x_0) = |C_f(x_0) W u_y(x = -x_0, y = 0) dx_0|$ where $C_f(x_0)$ represents the final contaminant concentration at the point where a water parcel exits the hyporheic zone (and enters the stream) and W represents the width of the stream. The average contaminant flux across the sediment–water interface can be found by substituting the EB flow model for u_y (eq 2c), adding up the net mass transferred ($m_{out}(x_0) - m_{in}(x_0)$) over all streamlines in the unit cell, and dividing by the interfacial area over which the mass is transferred:

$$J = \frac{u_m}{\pi} \int_0^{\pi/2} (-C_0 + C_f(\bar{x}_0)) \sin \bar{x}_0 d\bar{x}_0 \quad (5)$$

where $\bar{x}_0 = 2\pi x_0/\lambda$.

To solve this integral the final concentration $C_f(\bar{x}_0)$ must be specified. When all mass entering the hyporheic zone is lost by reaction (referred to here as the mass transfer-limit) the final concentration will be zero ($C_f(\bar{x}_0) = 0$) and eq 5 simplifies:

$$J_{MTL} = -\frac{C_0 u_m}{\pi} \quad (6)$$

The mass-transfer limited flux J_{MTL} represents the maximum mass flux that can be achieved by the EB model of hyporheic exchange; the negative sign in eq 6 indicates that the net mass flux is directed into the sediments.

Analytical Model of Hyporheic Exchange: Full Solution. In general, not all solute will react as a water parcel moves through the hyporheic zone. In such cases the final concentration will be greater than zero ($C_f(\bar{x}_0) > 0$) and the magnitude of mass flux across the sediment-water interface will be less than the mass-transfer limited case (i.e., $J/J_{MTL} < 1$). To solve this more general problem requires specification of the function $C_f(\bar{x}_0)$. If the solute in question is removed by first-order reaction then the final concentration will depend only on the time $\tau_f(\bar{x}_0)$ [T] it takes a water parcel to traverse the streamline that began at $\bar{x} = \bar{x}_0$:

$$C_f(\bar{x}_0) = C_0 e^{-k_r \tau_f(\bar{x}_0)} \quad (7)$$

where k_r [T^{-1}] is a first-order reaction rate constant.

To obtain an expression for the transit time function $\tau_f(\bar{x}_0)$ we exploit a surprising feature of the EB flow model: the x -component of the velocity is everywhere constant along the \bar{x}_0 streamline (eq 8, see proof in SI).

$$u_x(\bar{x}_0) = -u_m \cos \bar{x}_0 \quad (8)$$

The constancy of the x -velocity along a streamline can be understood by noting that near the sediment-water interface the modulus of the velocity vector is large but its x -component is small, whereas deeper into the sediment column the modulus of the velocity vector is small but its x -component is large (see Figure 1B). The constancy of $u_x(\bar{x}_0)$ implies that each streamline in the hyporheic zone can be analyzed as if it were a horizontal streamline beginning and ending at \bar{x}_0 and $-\bar{x}_0$, respectively, and through which mass is transported at a constant velocity $u_x(\bar{x}_0)/\theta$ (bottom highlighted streamline, Figure 1D). The residence time of a water parcel on the \bar{x}_0 streamline is therefore the ratio of the x -distance a fluid particle travels ($2x_0$) and its constant velocity in the x -direction:

$$\tau_f(\bar{x}_0) = \frac{2x_0}{-u_x(x_0)/\theta} = \frac{\lambda \bar{x}_0 \theta}{\pi u_m \cos \bar{x}_0} \quad (9)$$

Combining eqs 5, 7, and 9 we obtain a final expression for mass flux across the sediment–water interface:

$$J(\text{Da}) = J_{MTL} \left[1 - \frac{C_{exit}(\text{Da})}{C_0} \right] \quad (10a)$$

$$C_{exit}(\text{Da}) = C_0 \int_0^{\pi/2} \exp\left[-\frac{\text{Da} \bar{x}_0}{\pi^2 \cos \bar{x}_0}\right] \sin \bar{x}_0 d\bar{x}_0 \quad (10b)$$

$$\text{Da} = \frac{k_r \lambda \theta \pi}{u_m} \quad (10c)$$

The function C_{exit} is the flow-averaged concentration of contaminant exiting the hyporheic zone (and entering the stream)

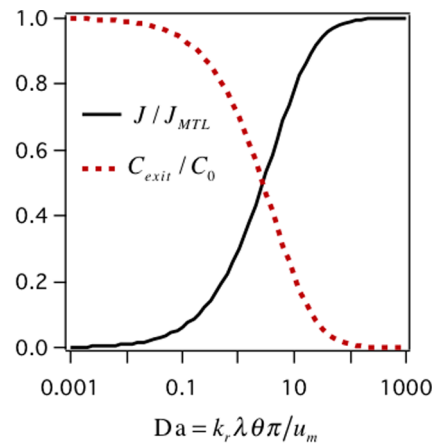


Figure 3. Model predictions of mass flux across the sediment-water interface (J) and flow-weighted concentration of contaminant exiting the hyporheic zone in an upwelling zone (C_{exit}) as a function of a nondimensional Damkohler Number, Da (see eqs 10a – 10c). The variables J_{MTL} and C_0 represent the mass-transfer-limited flux (eq 6) and fixed concentration of contaminant in the stream, respectively.

in an upwelling zone (proof in SI). The dimensionless Damkohler Number Da is the ratio of reaction rate to mass transport rate. According to our model, contaminant removal by hyporheic exchange and first-order reaction is fully determined by the value of Da (Figure 3). When the reaction rate is much slower than the mass transport rate ($Da < 0.01$) contaminants pass too quickly through the sediment to undergo reaction ($C_{\text{exit}}/C_0 = 1$) and the net mass flux across the sediment–water interface is zero ($J = 0$). When the reaction rate is much faster than the mass transport rate ($Da > 100$) contaminants undergo complete reaction ($C_{\text{exit}}/C_0 = 0$) and flux across the sediment–water interface is mass transfer limited ($J = J_{\text{MTL}}$). Between these two limits, mass flux across

$$\bar{C}(\bar{x}, \bar{y}, Da) = \frac{C(\bar{x}, \bar{y}, Da)}{C_0} = \exp\left[-\frac{Da(\cos^{-1}[e^{\bar{y}} \cos \bar{x}] - \bar{x})}{2\pi^2 e^{\bar{y}} \cos \bar{x}}\right], \quad -\pi/2 < \bar{x} < \pi/2, \bar{y} < 0 \quad (11)$$

This solution applies only within the single unit cell of the EB velocity field ($-\pi/2 < \bar{x} < \pi/2$). However, because all other unit cells are identical or mirror image, concentration in all other unit cells can be obtained from eq 11 by translation or reflection. Similar to the flux results presented earlier, contaminant concentration in the sediment pore fluids depends only on the value of the Damkohler Number. For the set of parameters listed in SI Table 1, the Damkohler Number is $Da = 2.2$ and the concentration field calculated from eq 11 is nearly identical to the concentration field generated from the numerical simulation (Figure 2B). The exception is in the upwelling zone near the sediment–water interface where the numerical simulation predicts a steep concentration gradient (see difference plot in Figure 2C). As noted earlier, this concentration gradient is an artifact of the constant concentration boundary condition imposed at the top of the numerical domain.

A Mass Transfer Coefficient for Hyporheic Exchange.

There is controversy in the literature regarding whether or not mass transfer coefficients can be used to model hyporheic exchange.^{21,22} Our solution sheds light on this issue. The solution for mass flux across the sediment–water interface (eq 10a) can be rearranged as follows:

$$J = -k_m(C_0 - C_{\text{exit}}) \quad (12a)$$

$$k_m = \frac{u_m}{\pi} \quad (12b)$$

The form of eq 12a is mathematically identical to a film model of interfacial mass transfer.²³ The driving force for mass transfer across the sediment–water interface is the difference in the flow-averaged concentration in downwelling (C_0) and upwelling (C_{exit}) zones. The quantity $k_m = u_m/\pi$ [$L T^{-1}$] represents the average volume of water per unit area (i.e., the Darcy flux) flowing into the sediment over a bed form.¹² The Damkohler Number introduced earlier can be written explicitly in terms of the mass transfer coefficient:

$$Da = k_r \lambda \theta / k_m \quad (13)$$

Several empirical approaches for estimating the mass transfer coefficient are described next.

Estimating the Mass Transfer Coefficient for Hyporheic Exchange. In this section we present several empirical approaches for estimating the mass transfer coefficient for hyporheic exchange. Because k_m is proportional to u_m

the sediment–water interface depends sensitively on the value of the Damkohler Number.

Comparison of Mass Flux Estimated by Numerical and Analytical Solutions. For the parameter values listed in SI Table 1, the average flux predicted from eq 10a, $J - (4 \times 10^{-7} \text{ ms}^{-1})C_0$, matches the average flux calculated from the numerical simulations presented earlier. Thus, the numerical and analytical solutions are in concordance.

Analytical Model of Hyporheic Exchange: Concentration Field. An exact solution for the concentration field in the sediment can also be derived for steady-state first-order reaction and advective transport through the hyporheic zone (see SI):

(see eq 12b), any empirical formula that relates u_m to stream state variables can also be used to estimate k_m . We evaluate two such expressions:

$$k_m^{\text{EB}} = 0.28 \frac{K_h U^2}{g \lambda} \left(\frac{\Delta/H}{0.34} \right)^\gamma, \quad \gamma = \begin{cases} 3/8 & \text{for } \Delta/H < 0.34 \\ 3/2 & \text{for } \Delta/H \geq 0.34 \end{cases} \quad (14a)$$

$$k_m^{\text{CW}} = K_h (a_1 + a_2 \text{Re}_\lambda^{b_1}), \quad \text{Re}_\lambda = \frac{U \lambda}{\nu}, \quad a_1 = 1.1 \times 10^{-5}, \\ a_2 = 1.45 \times 10^{-15}, \quad b_1 = 2.18 \quad (14b)$$

Equation 14a follows from a formula reported by EB¹² based on experiments conducted by Fehlman²⁴ which involved pressure measurements over artificial dunes submerged in a turbulent flow. Equation 14b follows from a formula proposed by Cardenas and Wilson (hereafter referred to as CW) based on numerical studies of turbulent flow over permeable dunes.¹⁵ Variables in these equations include the hydraulic conductivity K_h [$L T^{-1}$] of the sediments, stream velocity U [$L T^{-1}$] and depth H [L], bed form wavelength λ [L] and height Δ [L], gravitational acceleration g [$L T^{-2}$], and kinematic viscosity ν [$L^2 T^{-1}$].

To evaluate the empirical expressions above, mass transfer coefficients were calculated from 42 previously published hyporheic exchange experiments (reviewed in refs 25 and 26). Collectively, these experiments capture a variety of flow rates (0.09 to 0.5 m s^{-1}), bed form morphologies (ripples, dunes), sediment grain sizes (median values of 0.13–6 mm), and flume lengths (2.5–18.4 m).^{13,27–32} These experiments all had the same basic design. A recirculating flume is configured to mimic turbulent flow of water over a permeable sediment bed with periodic bed forms. A conservative (nonreactive and nonadsorbing) tracer is then added to the water column of the flume, and its concentration monitored over time. From mass balance, the instantaneous flux of tracer across the sediment–water interface can be calculated from the decline of tracer concentration (C_w) in the water column: $J = (V_w/A_s)(dC_w/dt)$ where the variables represent elapsed time t [T], the total volume (V_w [L^3]) of water overlying the sediment bed (including water in the recirculating pipes but excluding interstitial fluids in the sediment), and the surface area (A_s [L^2]) of the sediment–water interface. Mass-transfer-limited conditions are approximated at the very beginning of an experiment when $C_{\text{exit}} \approx 0$ (see eq 10a), and therefore a mass transfer coefficient can

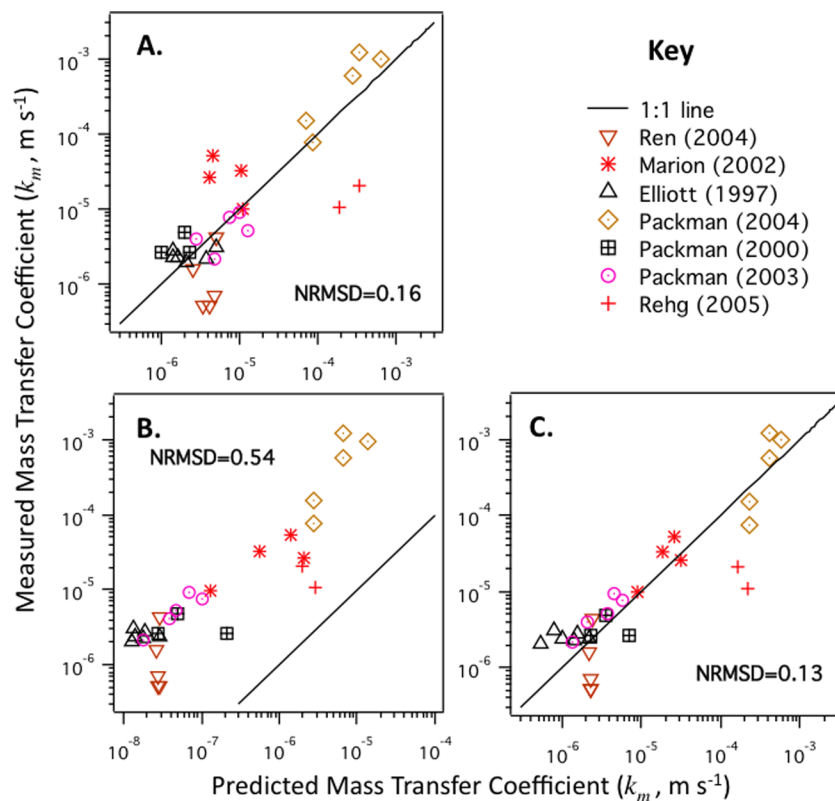


Figure 4. Measured versus model-predicted mass transfer coefficients for hyporheic exchange. Model-predicted mass transfer coefficients were calculated from (A) eq 14a proposed by Elliott and Brooks; (B) eq 14b proposed by Cardenas and Wilson; and (C) a modified form of the model proposed by Cardenas and Wilson (eq 14b with $a_1 = 0$, $a_2 = 2.51 \times 10^{-7}$, $b_1 = 0.85$).

be calculated from initial measurements of the instantaneous flux J_0 :

$$k_m^{\text{exp}} = -\frac{J_0}{C_0} \quad (15)$$

Equation 15 is obtained by combining eqs 6 and 12b and setting $J_{\text{MTL}} = J_0$.

Experimental mass transfer coefficients calculated from eq 15 range over 3 orders of magnitude from 5.2×10^{-7} to $5.8 \times 10^{-4} \text{ m s}^{-1}$. The EB formula (eq 14a) correctly predicts the magnitude and overall trend of these data, although some values are over- or under-predicted by up to a factor of 10 (Figure 4A, normalized root-mean-square deviance (NRMSD) of 16%, see SI for details of the NRMSD calculation). The CW formula (eq 14b) correctly reproduces the trend of the measured data, but consistently under-predicts their magnitude by approximately 10-fold (Figure 4B, NRMSD = 54%). The CW model can be made to fit the data by setting the constant $a_1 = 0$, and then performing a linear regression on the log-transformed k_m^{CW} and k_m^{exp} values ($a_1 = 0$, $a_2 = 2.51 \times 10^{-7}$, $b_1 = 0.85$) (Figure 4C, NRMSD = 13%). Of the three correlations evaluated here (EB, CW, and modified-CW), the EB best matches both the numerical simulations of hyporheic exchange through a triangular dune (see SI) and the trend and magnitude of measured mass transfer coefficients (Figure 4A). Therefore, the EB correlation (eq 14a) was adopted for estimating u_m from stream state variables in SI Table 1, and in the application of our model to contaminant removal in streams described later.

Model Limitations. Our analytical model's simplicity is both its strength and weakness. Stripping the problem to its essential elements (a canonical velocity field and first-order

reaction in the sediment) allows for explicit solutions for the flux and concentration fields, and provides a theoretical foundation for the application of mass transfer coefficients to the modeling and study of hyporheic exchange. However, in so doing we neglect many hydrological, biophysical, and chemical processes that can influence contaminant fate and transport in streams. First, the EB velocity field is an idealization of bed form pumping that simplifies many details of that process.^{11,15,16} Second, bed form pumping is only one of many transport mechanisms that can induce hyporheic exchange. Turbulent eddies in the water column of a stream, for example, can cause flow across the sediment-water interface in the presence or absence of bed forms.³³ Third, plants and animals colonizing the hyporheic zone can exert profound impacts on stream-sediment exchange, by forming mounds across which pumping occurs, inducing pore water flow within sediments, and structuring the permeability field with burrows and roots (reviewed in³⁴). Fourth, at a larger scale geomorphic features of a stream such as riffle-pool sequences, debris dams, meander bends, and regional groundwater flow all influence hyporheic exchange.^{1,2,35,36} Finally, many contaminants of practical interest are removed in the sediment by reactions and processes that do not conform to first-order kinetics.³⁷ Keeping these limitations in mind, below we utilize our simple model to evaluate the distances over which stream contaminants might be removed by hyporheic exchange through reactive sediments.

Evaluating the Distance over Which Contaminants Are Removed. The distance over which streamborne contaminants are removed can be estimated by combining our solution for flux across the sediment-water interface (eq 10a) with a steady-state model of streamflow where x is distance

along the stream and $C_{\text{stream},0}$ is the contaminant concentration in the stream at $x = 0$:

$$C_{\text{stream}} = C_{\text{stream},0} e^{-x/l} \quad (16a)$$

$$l = \frac{\lambda}{f_Q f_R} \quad (16b)$$

$$f_Q = \frac{u_m \lambda}{UH\pi} = \frac{k_m \lambda}{UH} \quad (16c)$$

$$f_R = \frac{J(\text{Da})}{J_{\text{MTL}}} \quad (16d)$$

In this model we assume: (1) steady state conditions; (2) down stream mass transport occurs by advection alone (i.e., longitudinal dispersion is neglected); (3) decline of contaminant concentration in the stream occurs over distances much larger than the wavelength of a single dune (i.e., contaminant concentration in the stream is constant over any single dune); and (4) any other in-stream processes (e.g., transient storage zones, decay in the water column) contribute negligibly to contaminant fate and transport. The parameter l represents the downstream distance over which contaminant concentration is significantly reduced (i.e., by the fraction $1/e$) due to hyporheic exchange and first-order reaction in the sediment bed. In the stream ecosystem literature, l is referred to as a “processing length”.³⁸ The fraction f_Q is the portion of stream discharge ($Q = UHW$) that flows through a single bed form ($u_m \lambda W/\pi$); the quantity f_Q/λ is therefore the fraction of stream discharge processed by the hyporheic zone per unit length of stream. The variable f_R represents the fraction of contaminant removed by first-order reaction as water flows through the hyporheic zone; its value can be calculated for any choice of the Damkohler Number (compare eqs 16d and 10a).

Minimizing the processing length l by manipulating stream state variables could provide the basis for design of constructed runoff or wastewater treatment systems.⁴ Similarly, river restoration plans could be designed to minimize l when contaminant removal within the hyporheic zone is a key objective,^{39–41} although this may need to be balanced with other objectives of hyporheic restoration.^{42,43} From eq 16b we deduce that decreasing l requires maximizing both f_Q/λ and f_R . Interestingly, these two fractions exhibit opposite dependencies on the mass transfer coefficient k_m . Increasing the mass transfer coefficient increases the fraction of streamwater processed by the hyporheic zone per unit length of stream ($f_Q/\lambda \propto k_m$) but reduces the time available for contaminants to undergo reaction in the hyporheic zone ($\text{Da} \propto 1/k_m$). The trade-off between reaction and transport implies that small changes in stream state variables can cause substantial changes in the processing length l . This can be demonstrated by writing f_Q/λ and Da explicitly in terms of state variables:

$$\frac{f_Q}{\lambda} = \frac{\delta K_h}{gH} \left(\frac{U}{\lambda} \right) \quad (17a)$$

$$\text{Da} = \frac{gk_r \theta}{\delta K_h} \left(\frac{\lambda}{U} \right)^2 \quad (17b)$$

where $\delta = 0.18$. Equations 17a and 17b are obtained by substituting the EB correlation for k_m (eq 14a) into the definitions

of f_Q/λ and Da , and assuming the dune height is $1/10$ the water depth, as is typically the case in natural streams.²⁸

For the set of stream state values used to generate Figure 2 (and listed in SI Table 1), the processing length calculated from eqs 17a, 17b, and 16b is very large ($l = 275$ km). Can this processing length be reduced by manipulation of stream characteristics? Because f_Q/λ depends inversely on H , decreasing water depth will decrease the processing length by a proportional amount. For example, a 5-fold decrease in water depth (from $H = 0.5$ to 0.1 m) will cause a 5-fold reduction in the processing length (from 275 to 55 km). For the set of values listed in SI Table 1, $f_R = 0.45$. Thus, an increase in k_r and/or θ will yield, at most, a 2-fold reduction in the processing length (from 275 to 138 km). Reach-averaged values of hydraulic conductivity typically range from 10^{-5} to 10^{-3} m/s [e.g., ref 44]. The value for K_h in SI Table 1 (9.81×10^{-4} ms⁻¹) is already near the upper end of that range, and therefore this state variable can only be decreased. Decreasing K_h by a factor of 10 increases the processing length by a factor of 5 from 275 to 1400 km. The variables U and λ have an opposite effect on f_Q/λ and Da . Decreasing the bed form wavelength (e.g., from $\lambda = 1$ to 0.1 m) increases the value of f_Q/λ by a factor of 10, decreases the value of Da by a factor of 100, and increases the processing length by a factor of 2.3, from 275 to 630 km.

The example calculations above illustrate how small changes in state variables can significantly alter the performance of hyporheic zone treatment systems. The calculations also reveal that engineered or natural hyporheic zone treatment systems operating outside their optimal state confer little water quality improvement over short distances (i.e., < 1 km). However, different empirical correlations for the mass transfer coefficient appear to give different predictions for the processing length. For example, when the modified CW correlation (eq 14b with modified coefficients) is used in place of the EB correlation (eq 14a), the predicted processing length is consistently shorter, in some cases by up to an order of magnitude. The different correlations also exhibit different degrees of agreement with numerical simulations of hyporheic exchange across triangular bed forms (see SI). Further research should focus on improving and field-testing empirical correlations for hyporheic exchange rates (k_m or equivalently u_m , see eq 12b), and developing more sophisticated quantitative models that can guide the experimental investigation and design of these low-energy natural treatment systems.

■ ASSOCIATED CONTENT

📄 Supporting Information

Numerical simulations, derivations, and figures. This material is available free of charge via the Internet at <http://pubs.acs.org>.

■ AUTHOR INFORMATION

Corresponding Author

*Phone: (949) 824-8277; fax: (949) 824-2541; e-mail: sbgrant@uci.edu.

Notes

The authors declare no competing financial interest.

■ ACKNOWLEDGMENTS

We thank A. McCluskey, P. Cook, E. Gee, M. Rippey and the anonymous reviewers for their comments and edits on the manuscript. The authors also gratefully acknowledge financial support from the U.S. National Science Foundation Partnerships

for International Research and Education (OISE-1243543) and an Australian Research Council Discovery Project (DP130103619).

REFERENCES

- (1) *The Hyporheic Handbook: A Handbook on the Groundwater-Surface Water Interface and Hyporheic Zone for Environmental Managers*, Integrated catchment science programme science report: SC050070; UK Environment Agency: Almondsbury, Bristol, 2009.
- (2) Krause, S.; Hannah, D. M.; Fleckenstein, J. H.; Heppell, C. M.; Kaeser, D.; Pickup, R.; Pinay, G.; Robertson, A. L.; Wood, P. J. Inter-disciplinary perspectives on processes in the hyporheic zone. *Ecology* **2011**, *4*, 481–499.
- (3) Hester, E. T.; Gooseff, M. N. Moving beyond the banks: Hyporheic restoration is fundamental to restoring ecological services and functions of streams. *Environ. Sci. Technol.* **2010**, *44*, 1521–1525.
- (4) Lawrence, J. E.; Skold, M. E.; Hussain, F. A.; Silverman, D. R.; Resh, V. H.; Sedlak, D. L.; Luthy, R. G.; McCray, J. E. Hyporheic zone in urban streams: A review and opportunities for enhancing water quality and improving aquatic habitat by active management. *Environ. Eng. Sci.* **2013**, *30*, 480–501.
- (5) Grant, S. B.; Litton-Mueller, R. M.; Ahn, J. H. Measuring and modeling the flux of fecal bacteria across the sediment-water interface in a turbulent stream. *Water Resour. Res.* **2011**, *47*, W05517 DOI: 10.1029/2010WR009460.
- (6) Hancock, P. J. Human impacts on the stream-groundwater exchange zone. *Environ. Manage.* **2002**, *29*, 763–781.
- (7) Wu, L.; Munoz-Carpena, R.; Gao, B.; Yang, W.; Pachepsky, Y. Colloid filtration in surface dense vegetation: Experimental results and theoretical predictions. *Environ. Sci. Technol.* **2014**, DOI: 10.1021/es404603g.
- (8) Monhanty, S. K.; Torkelson, A. A.; Dodd, H.; Nelson, K. L.; Boehm, A. B. Engineering solutions to improve the removal of fecal indicator bacteria by bioinfiltration systems during intermittent flow of stormwater. *Environ. Sci. Technol.* **2013**, *47*, 10791–10798.
- (9) Bardini, L.; Boano, F.; Cardenas, M. B.; Revelli, R.; Ridolfi, L. Nutrient cycling in bed form induced hyporheic zones. *Geochim. Cosmochim. Acta* **2012**, *84*, 47–61.
- (10) Huettel, M.; Berg, P.; Kotska, J. E. Benthic exchange and biogeochemical cycling in permeable sediments. *Annu. Rev. Mar. Sci.* **2014**, *6*, 23–51.
- (11) Janssen, F.; Cardenas, M. B.; Sawyer, A. H.; Dammrich, T.; Krietsch, J.; de Beer, D. A comparative experimental and multiphysics computational fluid dynamics study of coupled surface-subsurface flow in bed forms. *Water Resour. Res.* **2012**, *48*, DOI: 10.1029/2012WR011982.
- (12) Elliott, A. H.; Brooks, N. H. Transfer of nonsorbing solutes to a streambed with bed forms: Theory. *Water Resour. Res.* **1997**, *33*, 123–136.
- (13) Elliott, A. H.; Brooks, N. H. Transfer of nonsorbing solutes to a streambed with bed forms: Laboratory experiments. *Water Resour. Res.* **1997**, *33*, 137–151.
- (14) Rutherford, J. C.; Boyle, J. D.; Elliott, A. H.; Hatherell, T. V. J.; Chiu, T. W. Modeling benthic oxygen uptake by pumping. *ASCE J. Environ. Eng.* **1995**, *121*, 84–95.
- (15) Cardenas, M. B.; Wilson, J. L. Dunes, turbulent eddies, and interfacial exchange with permeable sediments. *Water Resour. Res.* **2007**, *43*, DOI: 10.1029/2006WR005787.
- (16) Thibodeaux, L. J.; Boyle, J. D. Bedform-generated convective transport in bottom sediment. *Nature* **1987**, *325*, 341–343.
- (17) Iversen, N.; Jorgensen, B. B. Diffusion coefficients of sulfate and methane in marine sediments: Influence of porosity. *Geochim. Cosmochim. Acta* **1993**, *57*, 571–578.
- (18) Bardini, L.; Boano, F.; Cardenas, M. B.; Sawyer, A. H.; Revelli, R.; Ridolfi, L. Small-scale permeability heterogeneity has negligible effects on nutrient cycling in streambeds. *Geophys. Res. Lett.* **2013**, *40*, 1118–1122.
- (19) Loffler, D.; Rombke, J.; Meller, M.; Ternes, T. A. Environmental fate of pharmaceuticals in water/sediment systems. *Environ. Sci. Technol.* **2005**, *39*, 5209–5218.
- (20) Hester, E. T.; Young, K. I.; Widdowson, M. A. Mixing of surface and groundwater induced by riverbed dunes: Implications for hyporheic zone definitions and pollutant reactions. *Water Resour. Res.* **2013**, *49*, 5221–5237.
- (21) Grant, S. B.; Marusic, I. Crossing turbulent boundaries: Interfacial flux in environmental flows. *Environ. Sci. Technol.* **2011**, *45*, 7107–7113.
- (22) Thibodeaux, L.; Valsaraj, K.; Reible, D. Letter to the editor regarding, “Crossing turbulent boundaries: Interfacial flux in environmental flows” *Environ. Sci. Technol.* **2012**, *46*, 1293–1294.
- (23) Cussler, E. L. *Diffusion: Mass Transfer in Fluid Systems*, 3rd ed.; Cambridge Series in Chemical Engineering, Cambridge, UK, 2009.
- (24) Fehlmann, J. M. Resistance components and velocity distributions of open channel flows over bedforms, M.S. Thesis; Colorado State University: Fort Collins, 1985.
- (25) Grant, S. B.; Stewardson, M. J.; Marusic, I. Effective diffusivity and mass flux across the sediment-water interface in streams. *Water Resour. Res.* **2012**, *48*, W05548 DOI: 10.1029/2011WR011148.
- (26) O'Connor, B. L.; Harvey, J. W. Scaling hyporheic exchange and its influence on biogeochemical reactions in aquatic ecosystems. *Water Resour. Res.* **2008**, *44*, DOI: 10.1029/2008WR007160.
- (27) Ren, J.; Packman, A. I. Stream-subsurface exchange of zinc in the presence of silica and kaolinite colloids. *Environ. Sci. Technol.* **2004**, *38*, 6571–6581.
- (28) Marion, A.; Bellinello, M.; Guymer, I.; Packman, A. Effect of bed form geometry on the penetration of nonreactive solutes into a streambed. *Water Resour. Res.* **2002**, *38*, DOI: 10.1029/2001WR000264.
- (29) Packman, A. I.; Salehin, M.; Zaramella, M. Hyporheic exchange with gravel beds: Basic hydrodynamic interactions and bedform-induced advective flows. *ASCE J. Hydraul. Eng.* **2004**, *130*, 647–656.
- (30) Packman, A. I.; Brooks, N. H.; Morgan, J. J. Kaolinite exchange between a stream and streambed: Laboratory experiments and validation of a colloid transport model. *Water Resour. Res.* **2000**, *36*, 2363–2372.
- (31) Packman, A. I.; MacKay, J. S., Interplay of stream-subsurface exchange, clay particle deposition, and streambed evolution. *Water Resour. Res.* **2003**, *39*, DOI: 10.1029/2002WR001432.
- (32) Rehg, K. J.; Packman, A. I.; Ren, J. Effects of suspended sediment characteristics and bed sediment transport on streambed clogging. *Hydrol. Processes* **2005**, *19*, 413–427.
- (33) Manes, C.; Pokrajac, D.; McEwan, I.; Nikora, V. Turbulence structure of open channel flows over permeable and impermeable beds: A comparative study. *Phys. Fluids* **2009**, *21*, 125109.
- (34) Meysman, F. J. R.; Galaktionov, O. S.; Cook, P. L. M.; Janssen, F.; Huettel, M.; Middelburg, J. J. Quantifying biologically and physically induced flow and tracer dynamics in permeable sediments. *Biogeosciences* **2007**, *4*, 627–646.
- (35) Hester, E. T.; Doyle, M. W. In-stream geomorphic structures as drivers of hyporheic exchange. *Water Resour. Res.* **2008**, *33*, DOI: 10.1029/2006WR0058.
- (36) Gomez, J. D.; Wilson, J. L.; Cardenas, M. B. Residence time distributions in sinuosity-driven hyporheic zones and their biogeochemical effects. *Water Resour. Res.* **2012**, *48*, DOI: 10.1029/2012WR012180.
- (37) Kessler, A. J.; Glud, R. N.; Cardenas, M. B.; Cook, P. L. M. Transport zonation limits coupled nitrification-denitrification in permeable sediments. *Environ. Sci. Technol.* **2013**, *47*, 13404–13411.
- (38) Fisher, S. G.; Grimm, N. B.; Marti, E.; Holmes, R. M.; Jones, J. B. Material spiraling in stream corridors: A telescoping ecosystem model. *Ecosystems* **1998**, *1*, 19–34.
- (39) Kaushal, S. S.; Groffman, P. M.; Mayer, P. M.; Striz, E.; Gold, A. J. Effects of stream restoration on denitrification in an urbanizing watershed. *Ecol. Appl.* **2008**, *18*, 789–804.

(40) Veraart, A. J.; Audet, J.; Dimitrov, M. R.; Hoffmann, C. C.; Gillissen, F.; de Klein, J. J. Denitrification in restored and unrestored Danish streams. *Ecol. Eng.* **2014**, *66*, 129–140.

(41) Hughes, R. M.; Dunham, S.; Maas-Hebner, K. G.; Yeakley, J. A.; Schreck, C.; Harte, M.; Molina, N.; Shock, C. C.; Kaczynski, V. W.; Schaeffer, J. A review of urban water body challenges and approaches: (1) Rehabilitation and remediation. *Fisheries* **2014**, *39*, 18–29, DOI: 10.1080/03632415.2013.836500.

(42) Boulton, A. J. Hyporheic rehabilitation in rivers: Restoring vertical connectivity. *Freshwater Biol.* **2007**, *52*, 632–650, DOI: 10.1111/j.1365-2427.2006.01710.x.

(43) Hester, E. T.; Gooseff, M. N. Hyporheic restoration in streams and rivers. In *Stream Restoration in Dynamic Fluvial Systems: Scientific Approaches, Analyses, and Tools*, Geophysical Monograph Series 194; American Geophysical Union, 2011; DOI: 10.1029/2010GM000966.

(44) Genereux, D. P.; Leahy, S.; Mitasova, H.; Kennedy, C. D.; Corbett, D. R. Spatial and temporal variability of streambed hydraulic conductivity in West Bear Creek, North Carolina, USA. *J. Hydrol.* **2008**, *358*, 332–353.